journal

Crack-Growth-Velocity-Dependent *R*-Curve Behavior in Lead Zirconate Titanate

Sergio L. dos Santos e Lucato[†]

Institute of Materials Science, Darmstadt University of Technology, 64287 Darmstadt, Germany

Crack-velocity (*v–K*) curves and crack-resistance (*R*) curves for unpoled ferroelectric and ferroelastic lead zirconate titanate (PZT) were determined for long cracks in compact-tension (CT) geometry using an *in situ* fracture device on the stage of an optical microscope. The steady-state crack length and the plateau value of *R*-curves measured at controlled constant velocities increased with increased velocity. The plateau value for 10^{-6} m/s was 1.2 MPa·m$^{1/2}$ after 1.3 mm of crack extension and for 10^{-4} m/s was 1.4 MPa·m$^{1/2}$ after 2.2 mm.

I. Introduction

CRACK growth can occur under conditions in which the applied load is less than the critical stress-intensity factor. Such behavior is known as subcritical crack growth and was first studied in glass.[1] Furthermore, in materials exhibiting a resistance curve (*R*-curve) behavior, a velocity dependence also has been found on the *R*-curve itself. Crack-velocity dependence in materials toughened by bridging has been investigated by measurement of *R*-curves at various loading rates.[2] Increasing crack-propagation velocity leads to a lower plateau value of the *R*-curve. The decrease in steady-state toughness is due to a change in the fracture mechanism from intergranular to transgranular with increasing velocity. Crack-velocity-curves (*v–K*-curves), with transformation toughening as process zone mechanism, display the three characteristic crack-velocity regimes found in glass, with the stress-intensity factors ranging over a large regime.[3] Ferroelastic switching, as it is found in some piezoelectric ceramics, is another process zone mechanism that exhibits subcritical crack growth.[4] In those materials, the crack-tip stress field leads to domain switching that exerts compressive stresses in the crack wake after crack growth and provides crack-tip shielding,[5–7] as shown schematically in Figs. 1(a) and (b). Furthermore, the subcritical crack growth is promoted by the presence of humidity, a feature common to many ceramics.[3,4,8,9]

A difficulty in the analysis of materials such as lead zirconate titanate (PZT) that exhibit a switching zone is that the switching zone width directly depends on the stress-intensity factor at the crack tip. The switching occurs only in a certain zone around the crack tip, where, in the absence of switching, the stresses are above a certain threshold (Figs. 1(a) and (b)). A high crack-propagation velocity requires high crack-tip *K*-level. High crack-tip *K*-levels signify high crack-tip stresses and lead to a large process zone,[10] which provides a high toughening effect. Thus, the externally applied load has to be increased to maintain a constant crack-tip

K-level. Otherwise, if the crack-tip *K*-level is changed during the measurement, the switching zone grows or shrinks, which invalidates the measurement. It is, therefore, crucial to maintain a constant-sized or steady-state zone, i.e., a constant *K*-level at the crack tip, throughout the measurement[3] by adjusting the applied load. Very little literature in this regard is available for ferroelastic materials.[4] In this communication, two procedures to accurately measure the *R*-curve and *v–K*-curve behavior in a material exhibiting ferroelastic toughening is introduced and their relevance demonstrated using PZT as a model material.

II. Experimental Methods

(1) Material and Specimen Preparation

All experiments were performed using a commercially available PZT (PI Ceramics, Lederhose, Germany). The specimens were delivered as unpoled plates of dimensions 50 mm × 48 mm × 3 mm and 35 mm × 33.6 mm × 3 mm. The specimens were polished on one side to a 1 μm finish and two holes were drilled for specimen fixture.

Before the measurements were taken, a sharp precrack was produced using a half-chevron notch and a Knoop indent with a load of 50 N, as described in Ref. 11. After the precrack had been driven through the region of the half-chevron notch, it was renotched to a final length of ∼50–150 μm.

(2) Crack Propagation

The compact-tension (CT) testing device was a new version of the type used before[11] and was mounted on the coordinate stage of an optical microscope. The crack length was obtained by targeting the crack tip with the crosshairs in the eyepieces of the microscope and reading out the value of the computerized coordinate stage. The applied load was measured using a 1 kN load cell connected
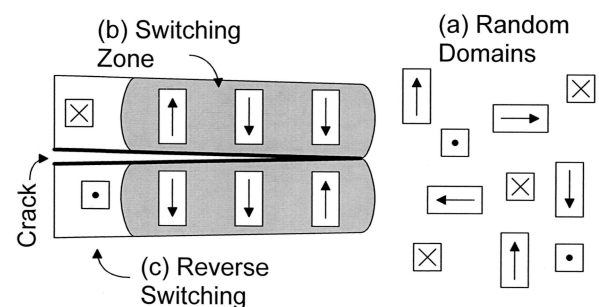
Fig. 1. (a) Development of a process zone by switching of initially unordered domains under the influence of the crack-tip stress field. (b) Increasing the applied stress-intensity factor increases the switching zone width and increases the crack-propagation velocity. Orientation of domains in the crack wake does not change as the crack grows and exerts compressive stresses. (c) Domains might switch back at the end of the crack wake, effectively decreasing the shielding.

through a measuring bridge. A piezoactuator was used to control the load applied to the specimen. The test itself was performed according to ASTM 399.[12] Even though the specimen thickness was less than required by ASTM 399, the equation for calculating the stress-intensity factor according to ASTM 399 was applied, because the size of the plastic zone in PZT was much smaller than the specimen thickness.

Two different procedures were used to record the crack length: applied load and crack-propagation velocity, depending on the crack-propagation velocity. For velocities $<10^{-5}$ m/s, the load-cell measuring bridge was connected to the computer digitally. A custom-designed software read the load value and the coordinates of the coordinate desk five times per second and calculated the applied stress-intensity factor. The data points consisting of the crack length, the applied load, and the time since the last data point were recorded by pressing a key.

Targeting the crack tip with the eyepieces yielded a very good accuracy but became difficult for crack-growth velocities $>10^{-5}$ m/s. Therefore, a video-based procedure was used. The analog output of the bridge was read by a second computer with an AD/DA card that generated a data bar with the applied load and time. This data bar was overlaid on the microscope video signal using a genlock, and the resulting video stream was recorded on a digital VCR. After the crack was run through the specimen, the video was analyzed frame by frame, and the applied load and the time were obtained from the data bar. The crack length was measured using a calibrated ruler on the video screen.

(A) R-Curves: Both procedures were used for the measurements of the *v–K*-curve and the *R*-curve, depending on the desired crack-propagation velocity. The *R*-curves were measured by loading the specimen to the desired crack-propagation velocity and then maintaining the velocity constant throughout the entire measurement. A spacing of ~25 μm between two data points was used at 10^{-6} m/s and a spacing of ~100 μm at 10^{-4} m/s up to a crack extension of 3 mm.

(B) v–K Curve Measurement: As mentioned earlier, the measurement of the *v–K*-curve requires more careful consideration because of the dependence of the switching zone size on the stress-intensity factor. The procedure used was as follows. Before the first data point was taken, the crack was extended by 500 μm at a velocity of 5×10^{-7} m/s to approach steady state. The actual data acquisition was divided in two phases. In the first phase, the crack was extended throughout the transient state to establish a constant switching zone size that corresponded to the crack-propagation velocity. The actual data acquisition immediately followed in the second phase. The first data point, consisting of the crack length, the applied load, and the time, was recorded after the transient state without stopping the crack. Three more data points were recorded after extension of the crack by a length Δa. The crack length Δa_{ss} to establish steady state was impractically high for low crack velocities, which required a pragmatic approach. Therefore, Δa_{ss} and Δa were slightly changed with crack-propagation velocity. Δa_{ss} was 500 μm for a crack velocity of $\geq 10^{-7}$ m/s, 300 μm for a crack velocity between 10^{-8} and 10^{-7} m/s, and 200 μm for a crack velocity $<10^{-8}$ m/s, while Δa was always 10% of Δa_{ss}. Special care was taken to ensure constant crack velocity during the entire data acquisition cycle. Finally, the crack velocity was calculated for two neighboring data points by dividing their distance by the time the crack required to propagate. The applied load and the crack length for that point were taken as the average of the two neighboring data points. Using this procedure, three interpolated data points ($\times$ in the Fig. 2 insert) were obtained form the four measured data points ($\bigcirc$ in the Fig. 2 insert) in each data acquisition cycle.

One data acquisition cycle was performed for each magnitude of velocity between 10^{-9} and 10^{-4} m/s. Two specimens were used in this measurement. The velocity of the first specimen was decreased by one magnitude in each cycle, which yielded a velocity range from 10^{-9} to 10^{-6} m/s. A velocity increment by one magnitude was performed in the second specimen to cover the range from 10^{-6} to 10^{-4} m/s. This procedure was needed to ensure that only small variations of the process zone size occurred from step to step. A similar technique, termed "load shedding," is used in metals. The
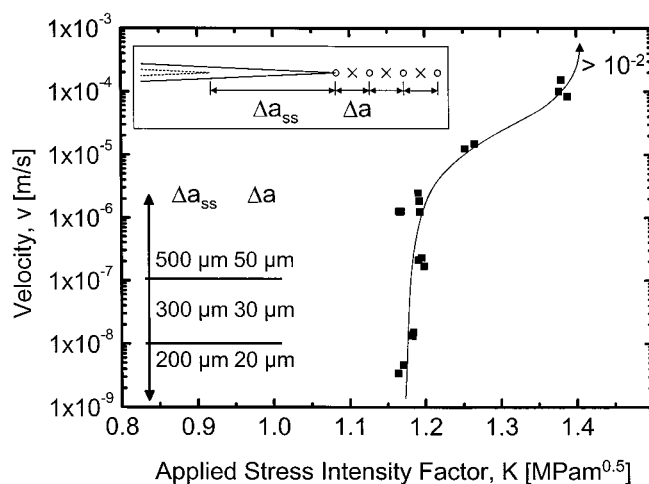

Fig. 2. *v–K*-curve for unpoled PZT material (line is only a guide to the eye and does not represent a fit to the data). Initial crack extension Δa_{ss} before a data point is taken and the distance between the data points Δa for a specific velocity is provided in the table.

ambient conditions in the laboratory throughout the entire measurement were of 24.4°–25.5°C and a relative humidity of 23%–26%.

III. Results and Discussion

(1) R-Curves

The measured *R*-curves and the corresponding crack-growth velocities are shown in Fig. 3. Because the specimens were not thermally depoled after the starter crack was grown, the initial value of the *R*-curves could not be measured with high precision. The *R*-curve measured at 10^{-6} m/s starts at ~0.8 MPa·m$^{1/2}$. A steep increase to 1.1 MPa·m$^{1/2}$ is observed in the first 400 μm of crack extension. The increase becomes a linear increase of the fracture toughness up to an extension of ~1.3 mm, after which the fracture toughness remains constant at 1.2 MPa·m$^{1/2}$. This final (steady-state) toughness value is termed "plateau." Assessment of the start value is more difficult at higher velocities because of the crack growth before a constant velocity can be adjusted. The steady-state region of the *R*-curve measured at 10^{-4} m/s commences at 2.2 mm with a corresponding stress-intensity factor of 1.4 MPa·m$^{1/2}$. The crack-growth velocity is maintained at 10^{-6} and 10^{-4} m/s with deviations of a factor of <3 in both experiments.

Increasing the crack-propagation velocity results in a higher plateau value and in a larger crack length required until the plateau
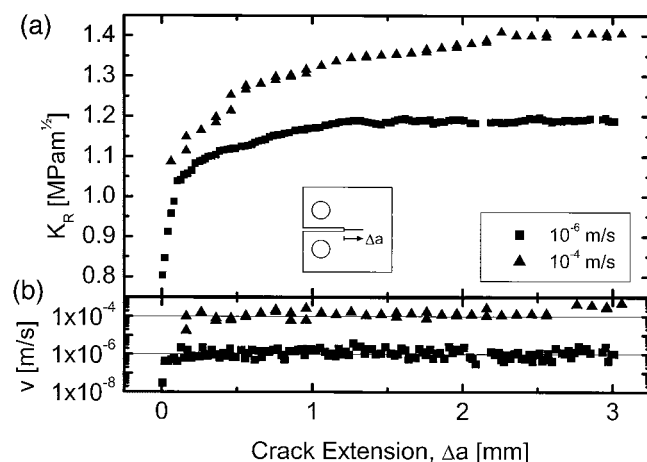

Fig. 3. (a) *R*-curve for two crack-growth velocities in unpoled PZT material. (b) Corresponding crack-growth velocity.

is reached. A higher crack-propagation velocity requires a higher stress-intensity factor, and, thus, the size of the switching zone is increased. This leads to an increased toughening effect and, thus, to a higher plateau value. The size of the switching zone also governs the steady-state crack length,[4] such that it is ~5 times the width of the switching zone. A wider switching zone thus leads to the larger crack length observed.

(2) v–K-Curve

The *v–K*-curve exhibits the three classically described regions.[1,3,4] Region I, which is characterized by a very strong dependence of the crack velocity on the stress-intensity factor, spans only from 1.1 to 1.2 MPa·m$^{1/2}$. Region II, with a small crack-velocity dependence on *K*, spans from 1.2 to ~1.4 MPa·m$^{1/2}$. The transition to region III is not well-defined, because the data are measured only for each magnitude of crack velocity; however, region III definitely starts at 1.4 MPa·m$^{1/2}$. A small increase of the applied load after the measurement at 10^{-4} m/s during the experiment leads to catastrophic failure of the specimen at a crack velocity $>10^{-2}$ m/s (given by the length of the ligament and the time between two video frames). The crack-propagation velocity of 10^{-6} m/s is measured in both specimens and results in good agreement between them.

In addition to the correlation between crack-tip stress and switching zone size, the use of a ferroelastic material introduces two additional complications. Domain switching is time dependent (crack-tip effect) and reversible (crack-wake effect). In case of a slowly growing crack, a higher fraction of domains in the switching zone initially switches, because the domains have more time to do so, which results in an increased toughness. On the other hand, more domains display reverse switching in the crack wake and, thus, decrease the toughening (Fig. 1(c)). For a rapidly growing crack, the two effects are reversed. Both effects can actually cancel each other, because they are opposite in sign and, therefore, decrease the influence of the crack-propagation velocity to a large degree.

IV. Conclusion

(1) *R*-curves at controlled constant crack-propagation velocities can be measured with high accuracy using long-crack measurements in PZT specimens in the CT geometry following the proposed procedures.

(2) The agreement between the plateau values of the *R*-curves measured at the two crack-propagation velocities and the corresponding stress-intensity factors in the *v–K*-curve is very good. The proposed procedure to measure a *v–K*-curve is, therefore, sufficient to ensure data acquisition always at the plateau.

(3) A larger transition length until steady state and a higher plateau value are observed for higher crack-propagation velocities in the *R*-curves. This is attributed to the increased size of the switching zone because of the increased stress-intensity factor at higher velocities.

References

[1]S. M. Wiederhorn, "Subcritical Crack Growth in Ceramics"; pp. 613–46 in *Fracture Mechanics of Ceramics*. Plenum, New York, 1974.

[2]S. Tandon and K. T. Faber, "The Influence of Loading Rate on Crack Bridging Process in Al$_2$O$_3$," *Acta Mater.*, **46** [10] 3547–55 (1998).

[3]M. C. Knechtel, D. E. Garcia, J. Rödel, and N. Claussen, "Subcritical Crack Growth in Y-TZP and Al$_2$O$_3$-Toughened Y-TZP," *J. Am. Ceram. Soc.*, **76** [10] 2681–84 (1993).

[4]S. W. Freiman, K. R. McKinney, and H. L. Smith, "Slow Crack Growth in Polycrystalline Ceramics"; pp. 659–76 in *Fracture Mechanics of Ceramics*. Plenum, New York, 1974.

[5]S. L. dos Santos e Lucato, D. C. Lupascu, and J. Rödel, "Effect of Poling Direction on *R*-Curve Behavior in Lead Zirconate Titanate," *J. Am. Ceram. Soc.*, **83** [2] 424–26 (2000).

[6]F. Meschke, A. Kolleck, and G. A. Schneider, "*R*-Curve Behaviour of BaTiO$_3$ due to Stress-Induced Ferroelastic Domain Switching," *J. Eur. Ceram. Soc.*, **17** [9] 1143–49 (1997).

[7]W. Yang, F. Fang, and M. Tao, "Critical Role of Domain Switching on the Fracture Toughness of Poled Ferroelectrics," *Int. J. Solids Struct.*, **38** [10–13] 2203–11 (2001).

[8]H. Wang, Y. Wang, Z. Jin, and H. Zhou, "The Effect of the Microstructure on the Static Fatigue Behaviour of Si$_3$N$_4$," *J. Mater. Sci.*, **32** [21] 5775–78 (1997).

[9]C. K. L. Davis, F. Guiu, M. Li, M. J. Reece, and R. Torrecillas, "Subcritical Crack Propagation Under Cyclic and Static Loading in Mullite and Mullite–Zirconia," *J. Eur. Ceram. Soc.*, **13** [3] 221–27 (1998).

[10]R. M. McMeeking and A. G. Evans, "Mechanics of Transformation Toughening in Brittle Materials," *J. Am. Ceram. Soc.*, **65** [5] 242–46 (1982).

[11]J. Rödel, J. F. Kelly, and B. R. Lawn, "*In Situ* Measurement of Bridged Crack Interfaces in the Scanning Electron Microscope," *J. Am. Ceram. Soc.*, **73** [11] 3313–18 (1990).

[12]"Standard Test Method for Plane-Strain Fracture Toughness of Metallic Materials," ASTM Designation E399–90, *Annual Book of ASTM Standards*, Vol. 3.03, pp. 407–37, ASTM International, West Conshohocken, PA, 1996. □